ISSN 0915-633X

NATIONAL INSTITUTE FOR FUSION SCIENCE

Bifurcation in Asymmetric Plasma Divided by a Magnetic Filter

K. Ohi, H. Naitou, Y. Tauchi, O. Fukumasa

(Received - May 14, 2001)

NIFS-699

May 2001

TOKI, JAPAN

Bifurcation in Asymmetric Plasma Divided by a Magnetic Filter

K. Ohi, H. Naitou*, Y. Tauchi, O. Fukumasa

Department of Electrical and Electronic Engineering,
Yamaguchi University, Tokiwadai 2-16-1, Ube 755-8611, Japan

Abstract

A magnetic filter (MF) reflecting electrons from both sides can separate a low-temperature and low-density subplasma from a high-temperature and high-density main plasma. The one-dimensional numerical simulation by the particle-in-cell code revealed that, depending on the asymmetry, the plasma divided by the MF behaves dynamically or statically [K. Ohi *et al.*, Physics of Plasmas **8**, 23 (2001)]. The transition between the two bifurcated states is discontinuous. In the dynamic state, the autonomous potential oscillation in the subplasma is synchronized with the passage of the shock wave structure generated by the modulated ion beam from the main plasma. The stationary phase of the dynamic state appears after the amplitude of the potential oscillation in the subplasma grows exponentially from the thermal noise. In the static state, the system is stable to the growth of the potential oscillation in the subplasma.

Keywords: magnetic filter, shock wave, limit cycle, PIC code, bifurcation, positive feedback, autonomous oscillation

*Guest staff of National Institute for Fusion Science, Toki, Gifu 509-5292, Japan (April 1, 1999 - March 31, 2001)

Bifurcation in Asymmetric Plasma Divided by a Magnetic Filter

K. Ohi, H. Naitou*, Y. Tauchi, O. Fukumasa

Department of Electrical and Electronic Engineering,
Yamaguchi University, Tokiwadai 2-16-1, Ube 755-8611, Japan

Abstract

A magnetic filter (MF) reflecting electrons from both sides can separate a low-temperature and low-density subplasma from a high-temperature and high-density main plasma. The one-dimensional numerical simulation by the particle-in-cell code revealed that, depending on the asymmetry, the plasma divided by the MF behaves dynamically or statically [K. Ohi *et al.*, Physics of Plasmas **8**, 23 (2001)]. The transition between the two bifurcated states is discontinuous. In the dynamic state, the autonomous potential oscillation in the subplasma is synchronized with the passage of the shock wave structure generated by the modulated ion beam from the main plasma. The stationary phase of the dynamic state appears after the amplitude of the potential oscillation in the subplasma grows exponentially from the thermal noise. In the static state, the system is stable to the growth of the potential oscillation in the subplasma.

Keywords: magnetic filter, shock wave, limit cycle, PIC code, bifurcation, positive feedback, autonomous oscillation

1 Introduction

A Magnetic filter (MF) is a localized magnetic field usually generated by the array of permanent magnets. The MF installed in the vacuum chamber can separate a plasma into two regions with different parameters. The transport of charged particles across the MF can be controlled by the properly selected strength of the MF due to the difference of the mass, the charge, and the energy[1, 2]. In this paper, the strength of the MF is chosen to reflect only electrons from both sides of the MF; it has little influence on ion dynamics because of large inertia. Due to thermal insulation of electrons by the MF, a subplasma with low density and low temperature can exist adjacent to a main plasma with high density and high temperature. It is to be noted that the potential gap created self-consistently at the MF can also have a crucial effect on particle dynamics across the MF. For the numerical study of asymmetric plasma divided by the MF, we used a visualized particle-in-cell simulation code in one dimension, VSIM1D[3], which runs on a PC-UNIX operating system and displays the real time portrayal of the phase space plots of charged particles and the potential profile, etc., on a monitor. The numerical investigation found the following interesting nonlinear phenomena[4, 5]: (1) Depending on the asymmetry, there are two bifurcated states; one is the static equilibrium state and the other is the dynamic state. (2) The dynamic state corresponds to the limit cycle (periodic attractor) in which the potential in the subplasma exhibits the autonomous oscillation synchronized with the passage of the shock wave structure caused by the modulated ion beam from the main plasma. (3) The transition between the states is the Hopf bifurcation from the stable equilibrium to the limit cycle. (4) The transition is discontinuous at the boundary (critical point).

The basic ideas to understand the physical picture underlying the above mentioned complex phenomena are described in the previous paper[5]. Measurements of the simulation results supported the validity of the ideas in some respects. This paper is intended to add more detailed measurements of the simulation results to confirm the ideas. Our concern is focused on the clues of the following two subjects. One is to explain the mechanism why the system exhibits autonomous oscillations in the dynamic state. The other is to elucidate the mechanism which makes the transition discontinuous.

This paper is organized as follows. An one-dimensional simulation model of the asymmetric plasma with the MF located at the center is described in Sec. 2. Simulation results are presented in Sec. 3. Conclusions and a discussion are given in Sec. 4.

2 Simulation Model

A simulation model employed in this paper is the same as the one described in Ref.[5]. The major differences in simulation parameters are the number of particles and the ion temperature. In order to reduce

*Guest staff of National Institute for Fusion Science, Toki, Gifu 509-5292, Japan (April 1, 1999 - March 31, 2001)

the thermal noise owing to the discreteness of particles, the number of particles used in the simulation is increased to four times as large as the one used in Ref.[5]. To observe the temporal evolution of the fine structure of the shock wave, the ion temperature is reduced by a factor of 1/4 lowering the ion sound speed $c_s = \sqrt{(T_e + 3T_i)/M_i}$ to enhance the Mach number. Here, T_e is the electron temperature, T_i is the ion temperature, and M_i is the ion mass.

Physical quantities are expressed in normalized units. The length is normalized by the grid size Δ. The time is normalized by the inverse of the electron plasma angular frequency ω_{pe}^{-1}, where ω_{pe} is defined by the initial average electron density in the main plasma. The normalized magnetic field strength is defined by ω_{ce}/ω_{pe}, where ω_{ce} is the electron cyclotron angular frequency. Temperatures and potentials are normalized by $m_e\Delta^2\omega_{pe}^2$ and $m_e\Delta^2\omega_{pe}^2/e$ with e and m_e being electron charge and mass, respectively. Full dynamics of electrons and ions are followed under the electrostatic approximation. Left and right boundaries of the system, $x = 0$ and $x = L_x = 400$, are grounded walls. Particles hitting the walls are absorbed there. The MF locates at the center of the system ($x = x_{MF} = 200$). The direction of the magnetic field is in the z-axis. The spatial profile of the magnetic field strength is given by

$$B(x) = B_0 \exp[\, -0.5(x - x_{MF})^2/a_{MF}^2 \,] \,.$$

where $B_0 = 0.5$ and $a_{MF} = 12$. The main plasma with $T_{Me} = 4$ and $T_{Mi} = 0.1$ exists in $x_{MF} \leq x \leq L_x$, whereas the subplasma with $T_{Se} = 1$ and $T_{Si} = 0.1$ exists in $0 \leq x \leq x_{MF}$. Here, T_{Me} and T_{Se} are electron temperatures, and T_{Mi} and T_{Si} are ion temperatures in the respective plasmas. Hydrogen plasma is assumed. Mass ratio is $m_i/m_e = 1836$. Time step size is $\Delta t = 0.2$. Four electrons and four ions are injected every one time step in the source region of the main plasma ($220 < x < 380$), while four electrons and four ions are inserted every N_{in} ($16 \leq N_{in} \leq 96$) time steps in the source region of the subplasma ($20 < x < 180$). Velocity distributions of electrons in the respective source regions are reset to form new Maxwellian distributions every 150 time steps. Without this artificial 'thermalization' process, the electron velocity distributions would be cooled down because only low energy electrons are confined by the sheath potential next to the walls.

3 Simulation Results

There are several control parameters governing the asymmetry of the plasma divided by the MF. In the previous paper, B_0 and N_{in}^{-1} are chosen for the control parameters. In this paper, N_{in}^{-1} is selected as the control parameter with a fixed value of B_0. Depending on the value of N_{in}^{-1} being proportional to the plasma production rate in the subplasma two bifurcated states are observed as in Ref.[5]. For $N_{in}^{-1} > 0.035$ the static state manifests. In the static state, the space potential of the subplasma is $\phi_S \sim 3T_{Se}$, while that of the main plasma is $\phi_M \sim 3T_{Me}$. Ions accelerated by the potential gap at the MF penetrates into the subplasma in which the ion beam component excites no instability. For $N_{in}^{-1} < 0.035$ the system behaves dynamically. The case of $N_{in} = 1/64$ is shown in Fig.1-5. Figure 1 expresses the temporal evolutions of the potentials at the centers of the main plasma and the subplasma, ϕ_M and ϕ_S, respectively. The potentials are time averaged over $\tau = 20$. In the stationary state at $t > 42000$, ϕ_S oscillates between $\sim 3T_{Se}$ and $\sim 3T_{Me}$, whereas ϕ_M is almost constant ($\phi_M \sim 3T_{Me}$) with small ripples synchronized with the oscillation of ϕ_S. The period of the autonomous oscillation is about 2170.

Figure 2 depicts a Lissajous figure of $\dot{\phi}_S$ (time derivative of ϕ_S), versus ϕ_S for $80000 \leq t \leq 160000$ (37 periods are included). In the terminology of nonlinear physics, the observed autonomous oscillation in the subplasma can be recognized as the limit cycle (periodic attractor) with the radius of $0.5\Delta\phi_s \sim 0.5(3T_{Me} - 3T_{Se})$, where $\Delta\phi_S$ is twice the amplitude of the oscillating part of ϕ_S. The upper bound of ϕ_S is limited by $\sim \phi_M \sim 3T_{Me}$; otherwise the direction of the ion flux crossing the MF will be changed. The lower bound of ϕ_S is determined by $\sim 3T_{Se}$ because loss of bulk electrons to the left wall in the subplasma will prevent ϕ_S from going down further.

Figure 3 displays snap shots of the potential and ion density profiles together with the phase space plots of ions for two different times in one period. In the phase space plots, red points indicate ions generated in the main plasma, whereas blue points denote ions born in the subplasma. Hence, the red points in the subplasma show ions coming from the main plasma. When the potential gap between two plasmas is large, the ion beam flux with high energy and high density gets into the subplasma from the main plasma and overtakes slower ions (see Fig.3(a)); the shock wave structure is formed. There is a sharp density peak in Fig.3(a) which corresponds to the shock front. The shock front observed in Fig.3(a) splits into two shock fronts as the shock wave structure propagates in the subplasma (see Fig.3(b)). The positions of the shock fronts are indicated by broken lines in Fig.3. The slight peaks of the potential profile are also found at the same positions of the density peaks in the subplasma. The ion density between the two shock fronts is higher than that of the ambient plasma. In Fig.3(b) the space potential of the subplasma is increased up to the level of the main plasma because of the intrusion of high-density ion beams. The faster shock front (head) reflects ions in front of the shock wave structure, while the slower shock front (tail) throws back ions at the rear of the shock wave structure. This shock wave structure is very similar to the one experimentally observed by Ikezi *et al.* [6]. They artificially excited the laminar shock wave in the double plasma machine by changing the potential gap between plasmas.

Figure 4 shows typical five periods of (a) poten-

tial variations at the center of the main plasma and the subplasma, ϕ_M and ϕ_S, (b) the ion flux Γ_i crossing the MF, (c) Γ_i hitting the left wall at $x = 0$, (d) the electron flux Γ_e hitting the left wall, and (e) the positions of the faster and slower shock fronts. The potentials in Fig.4(a) are extracted from Fig.1. The ion and electron fluxes shown in Fig.4(b)-(d) are measured by counting particles crossing the respective positions over $\tau = 20$. The quantities depicted in the ordinate in Fig.(b)-(d) are the number of counts per one normalized time divided by the initial number of ions (electrons) per one grid in the main plasma. The period of the limit cycle is determined by the transit time of the shock wave structure. The width between the shock fronts increases in time. The velocities of the faster and slower shock fronts determined by Fig.4(e) are $v_H = 0.088$ and $v_T = 0.062$, respectively. Hence, the Mach number for the respective shock fronts are $M_H = (v_H - v_{min})/c_s = 1.19$ and $M_T = (v_{max} - v_T)/c_s = 1.37$, where v_{max} and v_{min} are the maximum and minimum speed of the modulated ion beam. (In Ref.[5], it was difficult to distinguish the position of the faster shock front because $M_H \sim 1$.) Γ_i's crossing the MF and the left wall increase (decrease) as the potential gap increases (decreases). Γ_i hitting the left wall increases (decreases) suddenly when the faster (slower) shock front reaches the left wall. Γ_i hitting the left wall exists only when the region between two shock fronts is touching the left wall. When the potential in the subplasma is large, the electrons in the subplasma cannot arrive at the left wall because of the large sheath potential. It is clear that the shock wave structure approaching the left wall trigger the reduction of ϕ_S by pushing electrons (and ions) in front of the shock wave structure into the ion sheath without electrons. Hence, ϕ_S decreases just before the faster shock front hits the wall. The potential in the subplasma increases after the slower shock front reaches the wall because the ion flux behind the shock wave structure is smaller than the high-density ion flux accelerated by the large potential gap at the MF. Hence the formation of the shock wave structure is closely related to the mechanism underlying the limit cycle.

The mechanism approaching the stationary stage of the dynamic state can be explained in the following. Due to the thermal noise, the potential gap between the main plasma and the subplasma is modulated slightly. The weak shock wave structure, produced by the velocity modulated ion beam, propagates in the subplasma and reaches the left wall. If the reduction of the space potential caused by the approaching shock wave is bigger than that of the former potential modulation, the stronger shock wave will be formed. This process continues until the maximum potential of the subplasma goes up to $\sim \phi_M$. Time evolution of twice the amplitude of the oscillating part of ϕ_S in the transition stage, $\Delta\phi_S$, is presented in Fig.5. We can see that $\Delta\phi_S$ increases linearly in the transition stage. The growth rate obtained from Fig.5 is $\gamma = 0.96 \times 10^{-4}$. This growth rate is equivalent to the fact that one shock wave amplifies $\Delta\phi_S$ by a factor of 1.23 in every one transit time.

The N_{in}^{-1} dependence of γ in the transition stage is shown in Fig.6 as well as the N_{in}^{-1} dependence of $\Delta\phi_s$ in the stationary stage. The curve in Fig.6(b) is written from the data of γ in the dynamic state. When the autonomous oscillation is not observed (static state), we plotted the data as $\Delta\phi_s = 0$ and $\gamma = 0$. (At the moment it is very difficult to determine whether $\gamma = 0$ or $\gamma < 0$ in the static regime.) The positive values of $\Delta\phi_s$ and γ in Fig.6 correspond to the dynamic state. As the control parameter of N_{in}^{-1} reduces, the solution of this nonlinear system changes from the static state to the dynamic state of the limit cycle (Hopf bifurcation). The dynamic state of the limit cycle is observed for $N_{in}^{-1} \leq 1/29$, while the static state is seen for $N_{in}^{-1} \geq 1/28$. The critical point between the static state and the dynamic state is at $N_{in}^{-1} \sim 0.035$. We can see clearly that γ decreases to the value of zero when N_{in}^{-1} increases up to the critical point in which the transition is discontinuous. In the dynamic regime, as discussed in the previous paragraph, there is the positive feedback owing to the transit of the shock wave structure. In the static regime, we can expect that there is no positive feedback because bulk electrons mitigate the effect of the shock wave on the potential reduction when it approaches the left wall. The static state corresponds to the stable fixed point (attractor). As the control parameter of N_{in}^{-1} cross the critical point from the stable regime, the stable fixed point changes to the unstable one. So in the dynamic regime the solution of the nonlinear system moves from the unstable fixed point to the stable periodic attractor.

4 Conclusions and Discussion

The asymmetric plasma divided by the magnetic filter (MF) is numerically simulated. The one-dimensional particle-in-cell code VSIM1D[3] is used. The strength of the MF is chosen to reflect all electrons from both sides of the MF; ions move freely across the MF. Because of the thermal insulation of electrons by the MF, the low-temperature and low-density subplasma can exists adjacent to the high-temperature and high-density main plasma. The basic physics observed in this system are reported in Refs.[4, 5]. This paper has added detailed measurements to clarify the mechanism underlying the physics. We selected N_{in}^{-1}, which is proportional to the plasma production rate in the subplasma, as the parameter to control the asymmetry of the system. Depending on the asymmetry, the system behaves statically or dynamically. We have observed Hopf bifurcation at the critical point between the static regime and the dynamic regime; the stationary solution changes from the stable fixed point to the stable periodic attractor (limit cycle) as N_{in}^{-1} reduces. The transition between two bifurcated states is discontinuous at the boundary.

In the dynamic state, the electrostatic potential

in the subplasma ϕ_S shows the self-sustained oscillation. The minimum and the maximum of ϕ_S is $\sim 3T_{Se}$ and $\sim 3T_{Me}$ ($T_{Se} < T_{Me}$), respectively. The potential in the main plasma ϕ_M is almost constant ($\sim 3T_{Me}$) with small ripples synchronized with the autonomous oscillation in the subplasma. The modulated ion beam accelerated by the potential gap $\phi_M - \phi_S$ around the MF excites the shock wave in the subplasma. The shock wave structure has faster and slower shock fronts. The approaching faster shock front to the grounded wall has the effect to decrease ϕ_S because the electrons in front of the faster shock front is pushed into the electron-free ion sheath next to the wall. When the slower shock front is absorbed by the wall, ϕ_S starts increasing due to the difference between the smaller ion flux going into the wall and the larger ion flux coming into the subplasma across the MF.

The reason why the bifurcation is discontinuous at the critical point is explained as follows. We can assume that in the dynamic regime the initial state is the unstable fixed point and the solution of the system moves to the stable attractor. The picture is illustrated as follows. Due to the thermal noise, the potential gap is modulated slightly. The weak shock wave produced by the velocity modulated ion beam reaches the left wall. If the reduction of ϕ_S by the approaching shock wave is bigger than that of the former potential modulation, the stronger shock wave is formed. This positive feed back process continues until the maximum potential of the subplasma goes up to $\sim \phi_M$. The growth rate of the oscillating part of ϕ_S is measured in the dynamic regime. The growth rate decreases down to zero at the critical point as N_{in}^{-1} increases. In the static regime, there is no positive feedback because bulk electrons mitigate the effect of the approaching shock wave. So the threshold exists for the positive feed back to occur, which may be the ratio of the ion beam flux from the main plasma to the plasma density in the subplasma.

In this paper the control parameter is fixed during the temporal evolution of the simulation system. It is natural to expect that the system treated in this paper exhibits the hysteresis if the control parameter is changed very slowly. The hysteresis in the asymmetric plasma divided by the MF was studied in the separate paper[7].

Finally, we want to point out an application to the processing plasma. For the plasma etching of the semiconductor memory, charging of the dielectric substrate is critical because the potential structure formed at the substrate surface will deflect the ion flux accelerated by sheath potential adjacent to the substrate (anomalous etching). If the shock wave structures are autonomously excited in the processing reactor, the approaching shock waves will have the effect to neutralize the positively charged surface of the substrate. Hence, the etching speed may be enhanced drastically by keeping the directional character of the plasma etching.

Acknowledgement

The authors would like to express their thanks to Professors T. Kamimura, and K. Itoh, and H. Sanuki, National Institute for Fusion Science, Professor Y. Kawai, Kyushu University, and Professor K. Saeki, Shizuoka University, Professor Y. Ohsawa, Nagoya University for stimulating discussions. This work was supported in part by the Grant-in-Aid for Scientific Research from the Japanese Ministry of Education, Science, Sports and Culture.

References

[1] O. Fukumasa, H. Naitou, and S. Sakiyama, J. Appl. Phys. **74**, 848 (1993).

[2] O. Fukumasa, Y. Tauchi, and S. Sakiyama, J. Appl. Phys. **36**, 4593 (1997).

[3] K. Koga, H. Naitou, and Y. Kawai, J. Phys. Soc. Japan, **68**, 1578 (1999).

[4] H. Naitou, K. Ohi, and O. Fukumasa, Rev. Sci. Instrum. **71**, 875 (2000).

[5] K. Ohi, H. Naitou, Y. Tauchi, and O. Fukumasa, Physics of Plasmas **8**, 23 (2001).

[6] H. Ikezi, T. Kamimura, M. Kako, and K.E. Longgren, Phys. Fluids **16**, 2167 (1973).

[7] K. Ohi, H. Naitou, Y. Tauchi, O. Fukumasa, and K. Itoh, J. Plasma Fusion Res. SERIES (submitted).

Figure captions

Fig.1 Time evolutions of potentials at the center of the main plasma and the subplasma, ϕ_M, and ϕ_S. $N_{in}^{-1} = 1/64$.

Fig.2 Lissajous figure of the time derivative of ϕ_S versus ϕ_S. $N_{in}^{-1} = 1/64$.

Fig.3 Snap shots of spatial profiles of the electrostatic potential and the ion density (top), and phase space plots of ions (bottom) for two different times in one period. $N_{in}^{-1} = 1/64$.

Fig.4 Typical five periods of (a) electrostatic potentials at the center of the main plasma and the subplasma, ϕ_M, and ϕ_S, (b) the ion flux intruding the subplasma from the main plasma, (c) the ion flux entering the left wall, (d) the electron flux entering the left wall, and (e) the positions of the faster and slower shock fronts. $N_{in}^{-1} = 1/64$.

Fig.5 Time evolution of twice the amplitude of the oscillating part of ϕ_S, $\Delta\phi_S$, in the transition stage. $N_{in}^{-1} = 1/64$.

Fig.6 (a) $\Delta\phi_S$ versus $1/N_{in}$. (b) γ versus $1/N_{in}$. Here, $\Delta\phi_S$ is twice the amplitude of the oscillating part of ϕ_S in the stationary stage, and γ is the growth rate of $\Delta\phi_S$ in the transition stage.

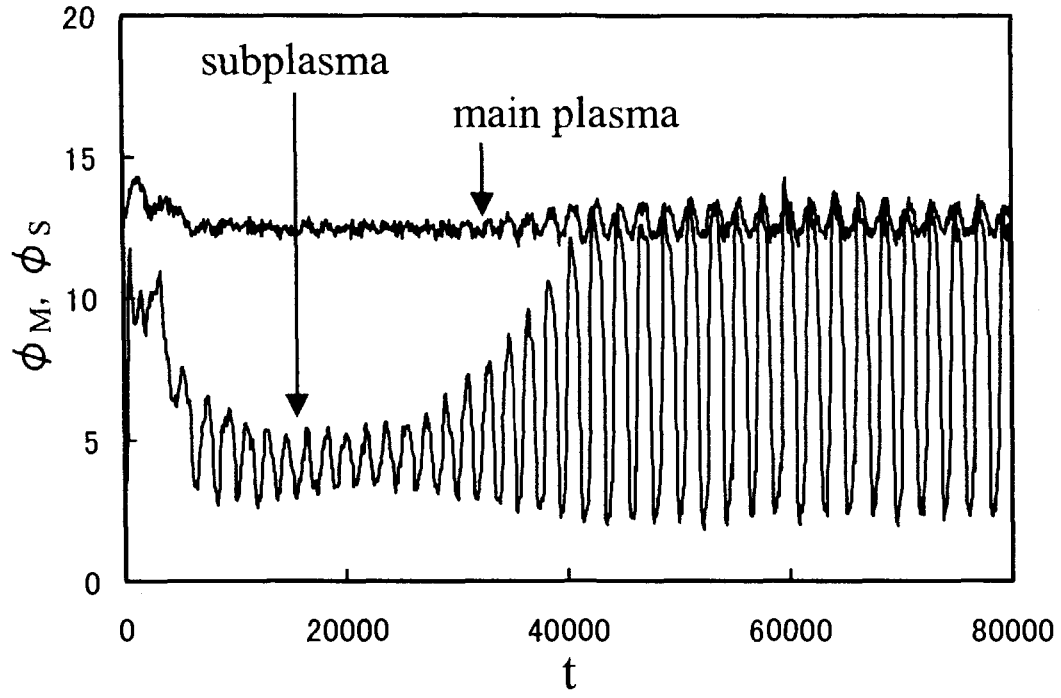
subplasma
main plasma
20
15
10
5
0
ϕ_M, ϕ_S
0
20000
40000
60000
80000
t

Fig.1

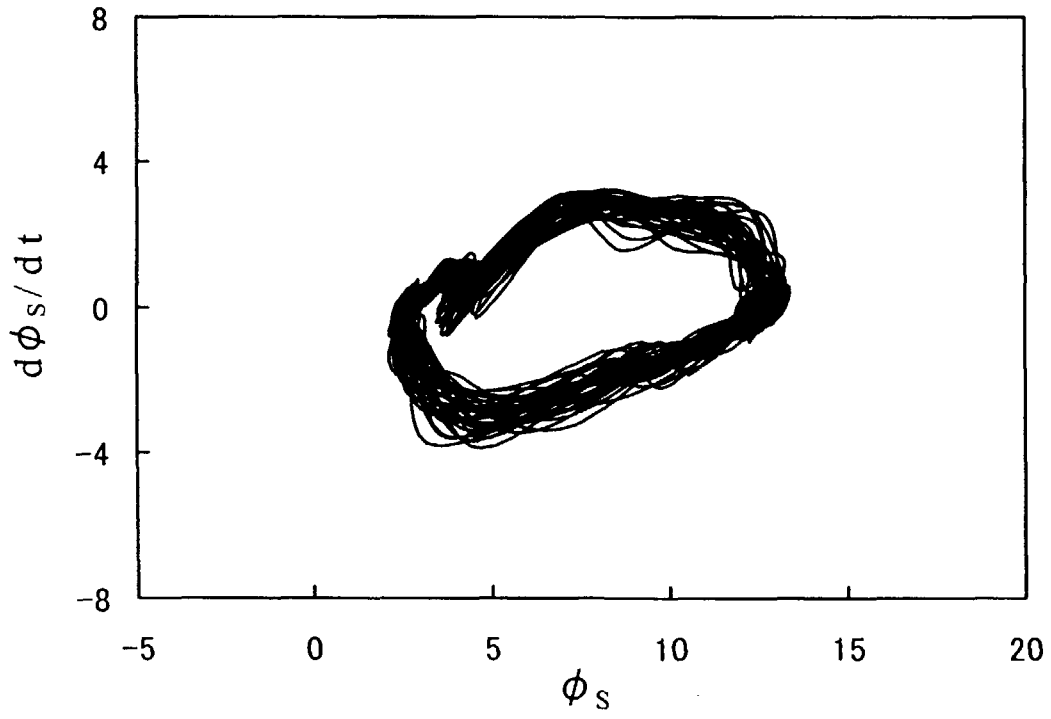
8
4
0
-4
-8
$d\phi_S/dt$
-5
0
5
10
15
20
ϕ_S

Fig.2

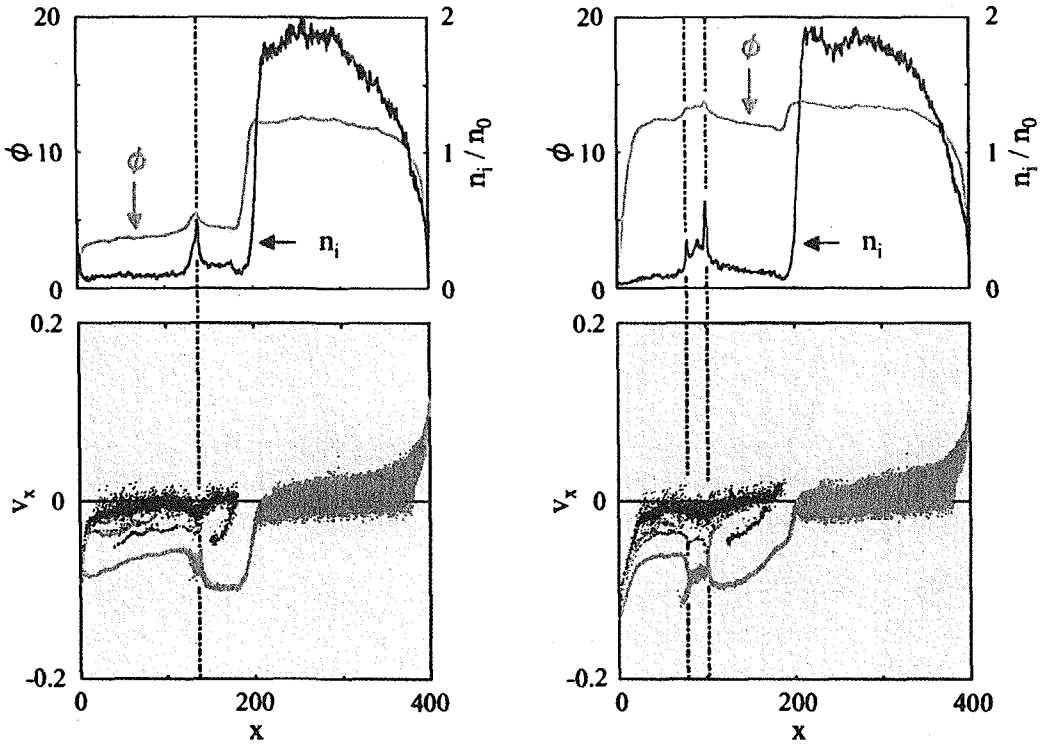

Fig.3

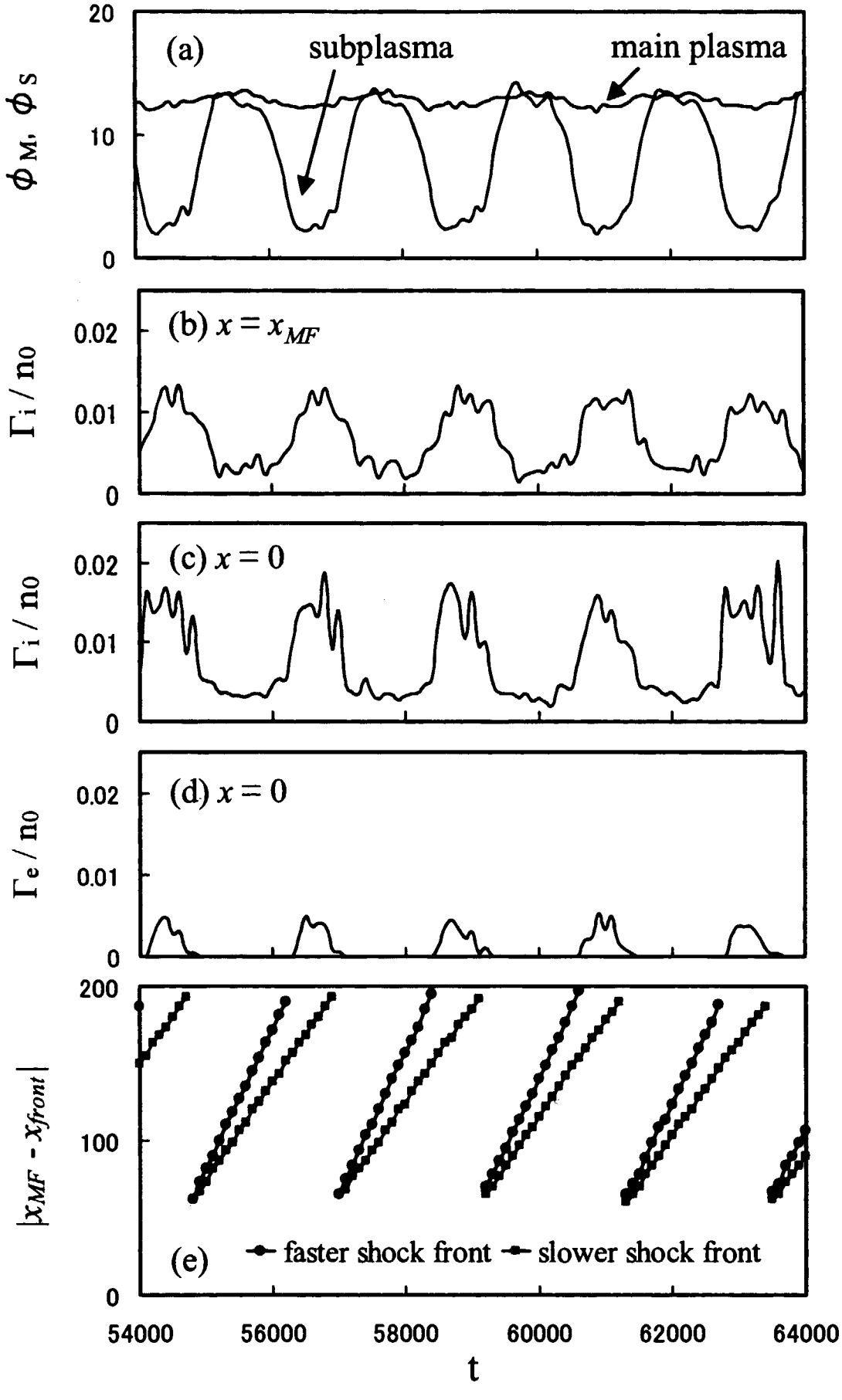
(a)
subplasma
main plasma
ϕ_M, ϕ_S
20
10
0
(b) $x = x_{MF}$
Γ_i / n_0
0.02
0.01
0
(c) $x = 0$
Γ_i / n_0
0.02
0.01
0
(d) $x = 0$
Γ_e / n_0
0.02
0.01
0
$|x_{MF} - x_{front}|$
200
100
0
(e)
faster shock front
slower shock front
54000
56000
58000
60000
62000
64000
t

Fig.4

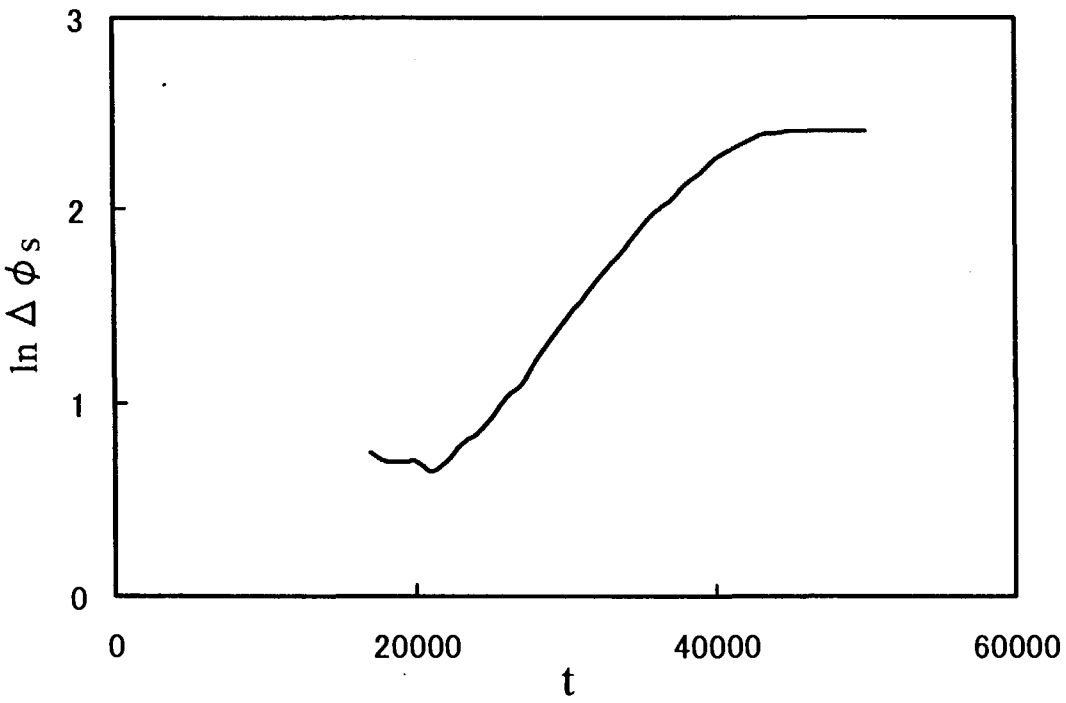

Fig.5

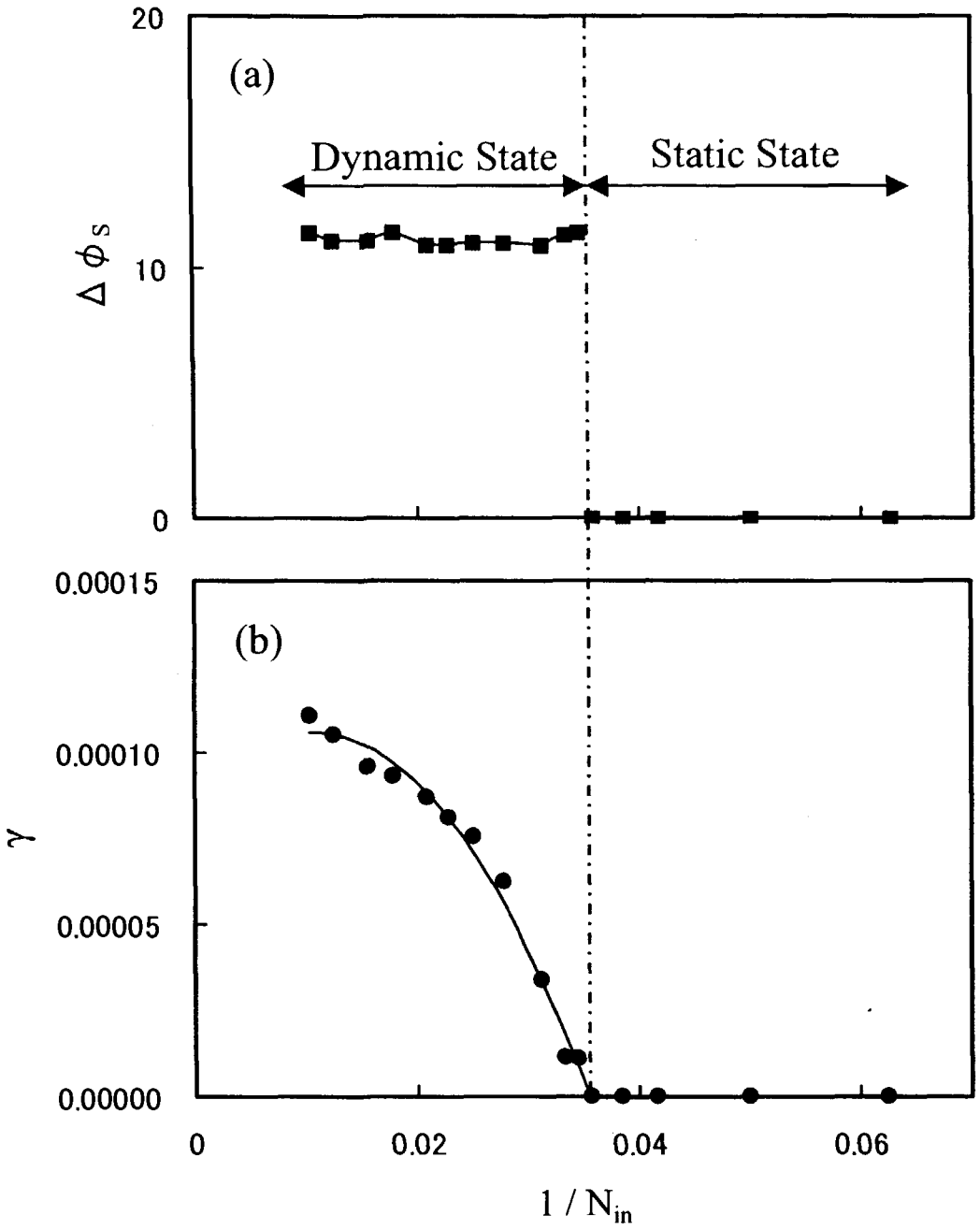
20
(a)
Dynamic State
Static State
Δ φs
10
0
0.00015
(b)
0.00010
γ
0.00005
0.00000
0
0.02
0.04
0.06
1 / Nin

Fig.6

Recent Issues of NIFS Series

NIFS-674 L.A. Bureyeva, V.S. Lisitsa and C. Namba,
Radiative Cascade Due to Dielectronic Recombination: Dec. 2000

NIFS-675 M.F.Heyn, S.V. Kasilof, W. Kernbichler, K. Matsuoka, V.V. Nemov, S. Okamura, O.S. Pavlichenko,
Configurational Effects on Low Collision Plasma Confinement in CHS Heliotron/Torsatron; Jan. 2001

NIFS-676 K. Itoh,
A Prospect at 11th International Toki Conference - Plasma physics, quo vadis?; Jan. 2001

NIFS-677 S. Satake, H. Sugama, M. Okamoto and M. Wakatani,
Classification of Particle Orbits near the Magnetic Axis in a Tokamak by Using Constants of Motion; Jan. 2001

NIFS-678 M. Tanaka and A. Yu Grosberg,
Giant Charge Inversion of a Macroion Due to Multivalent Counterions and Monovalent Coions: Molecular Dynamics Studyn; Jan. 2001

NIFS-679 K. Akaishi, M. Nakasuga, H. Suzuki, M.Iima, N. Suzuki, A. Komori, O. Motojima and Vacuum Engineering Group,
Simulation by a Diffusion Model for the Variation of Hydrogen Pressure with Time between Hydrogen Discharge Shots in LHD; Feb. 2001

NIFS-680 A. Yoshizawa, N. Yokoi, S. Nisizima, S.-I. Itoh and K. Itoh
Variational Approach to a Turbulent Swirling Pipe Flow with the Aid of Helicity; Feb. 2001

NIFS-681 Alexander.A.Shishkin
Estafette of Drift Resonances, Stochasticity and Control of Particle Motion in a Toroidal Magnetic Trap; Feb. 2001

NIFS-682 H. Momota and G.H. Miley,
Virtual Cathode in a Spherical Inertial Electrostatic Confinement Device; Feb. 2001

NIFS-683 K. Saito, R. Kumazawa, T. Mutoh, T. Seki, T. Watari, Y. Torii, D.A. Hartmann, Y. Zhao, A. Fukuyama, F. Shimpo, G. Nomura, M. Yokota, M. Sasao, M. Isobe, M. Osakabe, T. Ozaki, K. Narihara, Y. Nagayama, S. Inagaki, K. Itoh, S. Morita, A.V. Krasilnikov, K. Ohkubo, M. Sato, S. Kubo, T. Shimozuma, H. Idei, Y. Yoshimura, O. Kaneko, Y. Takeiri, Y. Oka, K. Tsumori, K. Ikeda, A. Komori, H. Yamada, H. Funaba, K.Y. Watanabe, S. Sakakibara, M. Shoji, R. Sakamoto, J. Miyazawa, K. Tanaka, B.J. Peterson, N. Ashikawa, S. Murakami, T. Minami, S. Ohakachi, S. Yamamoto, S. Kado, H. Sasao, H. Suzuki, K. Kawahata, P. deVries, M. Emoto, H. Nakanishi, T. Kobuchi, N. Inoue, N. Ohyabu, Y. Nakamura, S. Masuzaki, S. Muto, K. Sato, T. Morisaki, M. Yokoyama, T. Watanabe, M. Goto, I. Yamada, K. Ida T. Tokuzawa, , N. Noda, S. Yamaguchi, K. Akaishi, A. Sagara, K. Toi, K. Nishimura, K. Yamazaki, S. Sudo Y. Hamada, O. Motojima, M. Fujiwara,
Ion and Electron Heating in ICRF Heating Experiments on LHD: Mar. 2001

NIFS-684 S. Kida and S. Goto,
Line Statistics:Stretching Rate of Passive Lines in Turbulence: Mar. 2001

NIFS-685 R. Tanaka, T. Nakamura and T. Yabe,
Exactly Conservative Semi-Lagrangian Scheme (CIP-CSL) in One-Dimension : Mar. 2001

NIFS-686 S. Toda and K. Itoh,
Analysis of Structure and Transition of Radial Electric Field in Helical Systems : Mar. 2001

NIFS-687 T. Kuroda and H. Sugama,
Effects of Multiple-Helicity Fields on Ion Temperature Gradient Modes: Apr. 2001

NIFS-688 M. Tanaka,
The Origins of Elctrical Resistivity in Magnetic Reconnection: Studies by 2D and 3D Macro Particle Simulations: Apr. 2001

NIFS-689 A. Maluckov, N. Nakajima, M. Okamoto, S. Murakami and R. Kanno,
Statistical Properties of the Neoclassical Radial Diffusion in a Tokamak Equilibrium: Apr. 2001

NIFS-690 Y. Matsumoto, T. Nagaura, Y. Itoh, S-I .Oikawa and T. Watanabe,
LHD Type Proton-Boron Reactor and the Control of its Peripheral Potential Structure: Apr. 2001

NIFS-691 A. Yoshizawa, S.-I. Itoh, K. Itoh and N. Yokoi,
Turbulence Theories and Modelling of Fluids and Plasmas: Apr. 2001

NIFS-692 K. Ichiguchi, T. Nishimura, N. Nakajima, M. Okamoto, S.-i. Oikawa, M. Itagaki,
Effects of Net Toroidal Current Profile on Mercier Criterion in Heliotron Plasma: Apr. 2001

NIFS-693 W. Pei, R. Horiuchi and T. Sato,
Long Time Scale Evolution of Collisionless Driven Reconnection in a Two-Dimensional Open System; Apr. 2001

NIFS-694 L.N. Vyachenslavov, K. Tanaka, K. Kawahata,
CO2 Laser Diagnostics for Measurements of the Plasma Density Profile and Plasma Density Fluctuations on LHD Apr. 2001

NIFS-695 T. Ohkawa,
Spin Dependent Transport in Magnetically Confined Plasma; May 2001

NIFS-696 M. Yokoyama, K. Ida, H. Sanuki, K. Itoh, K. Narihara, K. Tanaka, K. Kawahata, N. Ohyabu and LHD experimental group
Analysis of Radial Electric Field in LHD towards Improved Confinement; May 2001

NIFS-697 M. Yokoyama, K. Itoh, S. Okamura, K. Matsuoka, S. -I. Itoh,
Maximum-J Capability in a Quasi-Axisymmetric Stellarator; May 2001

NIFS-698 S-I. Itoh and K. Itoh,
Transition in Multiple-scale-lengths Turbulence in Plasmas; May 2001

NIFS-699 K. Ohi, H. Naitou, Y. Tauchi, O. Fukumasa,
Bifurcation in Asymmetric Plasma Divided by a Magnetic Filter; May 2001